

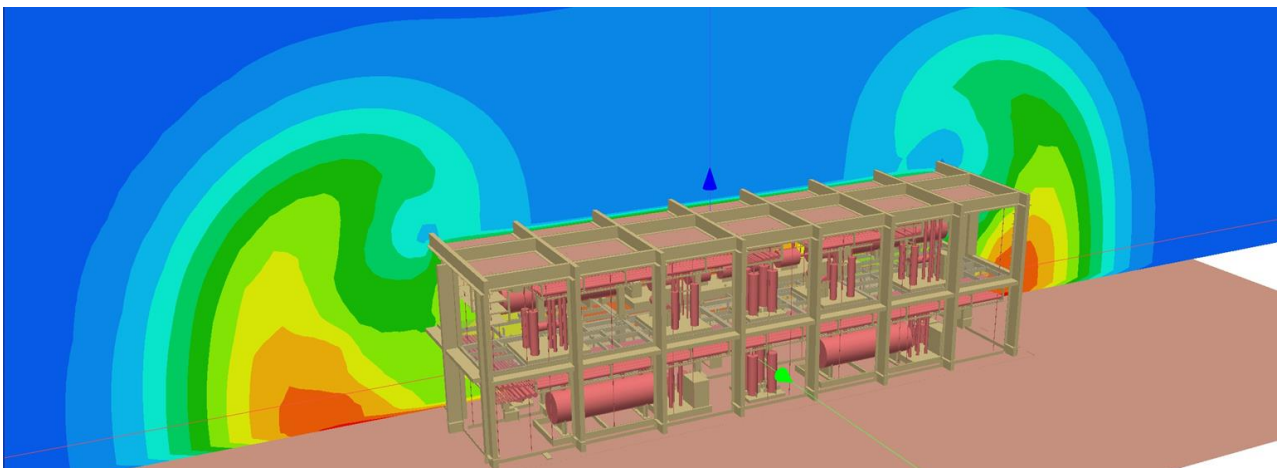


Validation Summary

EXSIM

VERSION: 6.0

DATE: March 2023





Reference to part of this report that may lead to misinterpretation is not permissible.

No.	Date	Reason for Issue	Prepared by	Verified by	Approved by
1	March 2023	First issue	J Thompson	BE Vembe	T Evanger

Date: March 2023

Prepared by: Digital Solutions at DNV

© DNV AS. All rights reserved

This publication or parts thereof may not be reproduced or transmitted in any form or by any means, including copying or recording, without the prior written consent of DNV AS.

Table of contents

1	INTRODUCTION.....	2
1.1	Overview	2
1.2	Scope and objectives	2
1.3	Report structure	2
2	METHODOLOGY.....	3
2.1	Approach	3
2.2	Identification and gathering of experimental data	3
2.3	Modelling	3
2.4	Results extraction and analysis	4
2.5	Calculation of statistical measures and confidence limits	4
3	VALIDATION CASES.....	7
3.1	Case summary	7
3.2	SOLVEX	8
3.3	Troll Process Module	12
3.4	CMI Offshore Compressor (M24) and Separator (M25) Modules	14
3.5	DNV Module	18
3.6	BFETS Phase 3A	21
3.7	BFETS Phase 3B (full scale tests)	26
3.8	DNVGL Explosion Chamber	30
3.9	Shell/HSL hydrogen repeated pipe congestion	33
3.10	FM Global vented hydrogen explosion tests	36
4	SUMMARY OF MODEL PERFORMANCE	40
5	REFERENCES.....	41



1 INTRODUCTION

1.1 Overview

Model validation is a process by which the predictive capabilities of a model (within the bounds of its intended use) are systematically evaluated against independent real-world observations/data. Alongside establishing the expected prediction accuracy of the model, the validation process provides the additional benefit of creating reference points against which the merits of candidate modifications/updates can be evaluated.

In this technical report, the work undertaken and results obtained from the latest validation exercise performed for the EXSIM gas explosion simulator are presented and discussed.

1.2 Scope and objectives

The gas explosion simulation code EXSIM has been subjected to extensive validation efforts over its 30+ year history [1-8]. However, until now, much of the publicly available work has been particular to (now) superseded versions of the code. The aim of the present document is to address this issue by providing users (and other stakeholders) with a single, comprehensive, referenceable validation document for the current version of the simulator (6.0, the latest build at the time of writing).

1.3 Report structure

The document is structured as follows:

Section 1.0 Introduction

Section 2.0 Methodology

A high-level description of the assessment methodology is provided in this section, including details of the assessed quantities (i.e., the model outputs used for comparison against experimental measurements) and the statistical measures selected to assess model performance.

Section 3.0 Validation Cases

In this section, overviews of the various experimental programmes used in support of the validation exercise are presented on a case-by-case basis, along with model setup details and, finally, the obtained results.

Section 4.0 Summary of Model Performance

A summary of the model's overall performance against the full validation data library is provided in this section.

Section 5.0 References

2 METHODOLOGY

2.1 Approach

Due to their inherent complexity, Computational Fluid Dynamics (CFD) models such as EXSIM do not lend themselves well to traditional approaches of appraising model uncertainty (e.g., individually assigning uncertainties to all model components and propagating these distributions through the system to yield an overall uncertainty estimate). Accordingly, the EXSIM validation campaign presented herein has been based on the model evaluation framework set out by Hanna *et al.* [9], which is broadly aligned with the method suggested in the Gas Explosion Model Evaluation Protocol (MEGGE) [10]. In summary, the adopted approach entails direct comparison of the model's predictions with a broad range of experimental data in combination with application of a series of statistical measures to yield an overall view of model performance – see Figure 1.



Figure 1: Outline of model evaluation approach

High-level descriptions of each step are provided in the following sub-sections.

2.2 Identification and gathering of experimental data

The first step of the model evaluation procedure involves identifying relevant experimental campaigns and gathering the associated outputs necessary for constructing equivalent EXSIM models in support of the assessment (summary reports, time history data etc.).

The experimental data supporting the current work were drawn from a variety of sources, including both those published in the open literature (journal articles, technical reports, conference papers/presentations etc.) and DNV's internal database. The search was targeted to ensure that the selected library of experimental works, considered together, covered a broad range of parameters pertinent to explosion hazards, including congestion and confinement levels, ignition locations and fuel types. A summary of the selected cases is provided in Section 3.

2.3 Modelling

In this step, EXSIM models are constructed and run for each identified experiment listed in the case library developed in the previous stage.

For the current work, the latest release of EXSIM, version 6.0, was used for the entirety of the validation programme. Whilst the modelling results reported herein were obtained from the Linux compatible build of the code, similar results would be obtained for the Windows build (as confirmed by spot-testing).

The overall modelling process for the current work proceeded as follows:

- Construction/importing of 3D geometry
- Selection of fuel type
- Setting of ignition type and location
- Building of computational mesh
- Setting of boundary conditions

- Specification of required outputs and monitoring locations (see discussion in Section 2.4)
- Specification of simulation stop criteria
- Running of simulation

Specific details of the inputs used at each stage of the modelling process are provided on a case-by-case basis in Section 3. The aim is to provide sufficient detail to enable users to fully reconstruct each case.

To ensure consistency, and fair comparison of the outcomes that would be obtained from 'best practice' use of the code, all reported cases were modelled based on the guidelines set out in the EXSIM user guide [11]. Accordingly, as is standard practice for EXSIM simulations, meshing of the core combustion regions for the 'base case' models was performed in all instances in alignment with the recommendations made by the companion EXSIMPOR utility. Similarly, the Courant numbers controlling the solution's time-stepping were set to default values (calculated at runtime by the simulator) throughout.

Finally, with efficiency in mind, the stop criteria were typically tuned for each case to optimise the simulation times – in general, these would be set to terminate the simulations shortly after the initial pressure peaks were recorded at each monitoring location. Where such optimisation was not performed, simulations were typically set to terminate when 90% of the fuel in the simulation domain had been consumed.

2.4 Results extraction and analysis

The next step of the methodology involves the extraction and post-processing of the simulation results, followed by comparison with the corresponding experimental data.

For the current version of the validation report, the assessment is limited to comparison of predicted and observed peak overpressures¹. In general, where possible, point-by-point comparisons for all *internal* pressure transducers are provided alongside comparisons of the *maximum peak pressure* recorded across the entire group (hereafter referred to as the 'max. of peak' pressure).

Where possible, the experimentally recorded pressure data were smoothed using an appropriate rolling average (approx. 1-2 ms) to remove short duration spikes that could misrepresent the recorded pressures; whilst this treatment is known to typically yield a slight reduction in the associated peak pressures, such short-lived pressure spikes would be unlikely to make a significant contribution to the overall impulse or, by extension, any resultant structural response.

For instances wherein specific experiments are repeated within a given test series, the result was taken as the mean average reading.

2.5 Calculation of statistical measures and confidence limits

As recommended in the MEGGE, the final step of the process involves extending the direct comparisons between prediction and observation performed in Step 2 by means of statistical analysis.

2.5.1 Statistical performance measures

The selection of performance measures for the present work was based on the desire to indicate whether the model (in the general case) over- or underpredicts and, secondly, indicate the level of scatter in the model's predictions.

Considering the above requirements in tandem with the propensity for predicted and observed pressures within a given series of experiments to span several orders of magnitude, the following three commonly used fundamental measures were selected in support of the assessment:

- Geometric Mean Bias (MG)

¹ In subsequent editions, it is intended for this to be extended to include flame arrival times and (where possible) impulses.

- Geometric Variance (VG)
- Fraction of Predictions Within a Factor of Two of Observed Values (FAC2)

Brief descriptions of each measure, including indicative value ranges that correspond to a 'good model', are presented below.

2.5.1.1 Geometric mean bias (MG)

The geometric mean bias (*MG*) provides a measure of the systematic error in a model's predictions that will lead to consistent over- or underprediction, and is defined as follows:

$$MG = e^{\left(\overline{\ln\left(\frac{C_o}{C_p}\right)}\right)} \quad (1)$$

Where:

C_o is the experimentally observed value

C_p is the predicted value

The overbar indicates the mean average over all pairs of sample points (C_o and C_p)

As *MG* is based on the natural logarithm of the quantity of interest, it lends itself well to datasets spanning multiple decades. For a 'perfect' model, $MG = 1.0$ whilst values of $MG = 0.5$ and $MG = 2.0$ indicate a model that over- or underpredicts by a factor of two, respectively. As a guide, Chang and Hanna [12] suggest that a 'good' model² would be characterised by a mean bias within $\pm 30\%$ of the mean i.e. $0.7 < MG < 1.3$.

2.5.1.2 Geometric variance (VG)

The second of the adopted measures, the geometric variance (*VG*), indicates the degree of scatter in the model's predictions due to a combination of both systematic and random errors, and is given by:

$$VG = e^{\left(\overline{\ln\left(\frac{C_o}{C_p}\right)^2}\right)} \quad (2)$$

As per the mean bias expressed above, *VG* is based on the natural logarithm of the quantity of interest and therefore suited to strongly varying datasets. $VG = 1.0$ for a 'perfect' model and, according to Chang and Hanna, a 'good' model should be expected to achieve a random scatter within a factor of 2 to 3 of the mean (i.e. $VG < 3.3$).

2.5.1.3 Fraction within a factor of two (FAC2)

Completing the set of the selected performance measures is the fraction of predictions whose values lie within a factor of two of the observed values (*FAC2*). The *FAC2* measure offers the particular advantage that it is not excessively influenced by outliers in the dataset.

It naturally follows that $FAC2 = 1.0$ for a 'perfect' model; for a 'good' model, Chang and Hanna suggest that more than half of the predicted values should be within a factor of two of their observed counterparts (i.e. $FAC2 > 0.5$).

2.5.2 Confidence limits

Finally, confidence limits are calculated for *MG* to yield an indication of the degree of uncertainty associated with the estimate of the true mean bias. For this, the bootstrap resampling procedure described by Efron [13] is employed to determine the confidence limits. A particular advantage of this approach is that it does not require any specific assumptions to be made regarding the distribution of the data (the commonly adopted 'Student t' procedure, for example, presupposes that the assessed data follows a normal or Gaussian distribution).

For the present work, the 95% confidence interval (CI) for *MG* is calculated and reported. It should be noted that this does not indicate that there is 95% confidence that the true *MG* lies within the quoted range; a more accurate interpretation

² Whilst it is recognised that the work of Chang and Hanna is specific to atmospheric dispersion models, their suggested values are considered to provide a reasonable guideline for the present analysis.

would be that, if repeat random samples were taken and associated confidence intervals were calculated, the ‘true’ MG would lie within the quoted range 19 times out of 20 (on average).

2.5.3 Results presentation

For each validation case, both tabulated and graphical summaries of model performance are provided as follows:

- Tabulated summaries of the selected fundamental performance measures (MG , VG and $FAC2$)
- Scatter plots of C_o against C_p
- Scatter plots of MG against VG

A representative C_o vs. C_p scatter plot is shown in Figure 2 (left pane). Here, points lying on the solid line indicate perfect agreement between the model’s predictions and the experimentally observed values; points lying within the band bounded by the two dashed lines indicate agreement within a factor of two.

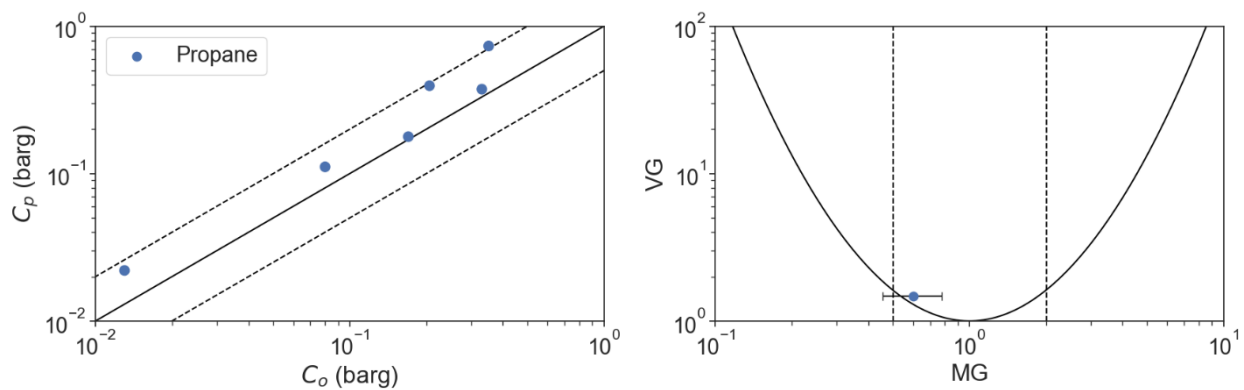


Figure 2: Example scatter plots of C_o vs. C_p (left pane) and MG vs. VG (right pane). In this example, the results indicate a model that tends to overpredict slightly.

A representative MG vs VG scatter plot is presented in Figure 2 (right pane). Included in the plot (and all such plots) is a solid parabola indicating the minimum theoretical variance as a function of mean bias:

- A ‘perfect’ model would be indicated by a point at the basin of the parabola (i.e. $MG = 1.0$ and $VG = 1.0$)
- Models with points that lie on the parabola (above or below $MG = 1.0$) are observed to over- or under-predict consistently by a similar factor
- Finally, models with points that lie above the baseline defined by the parabola will over- and underpredict by a similar factor (relative to the mean bias)

Also included in plots of this type are dashed lines at $MG = 0.5$ and $MG = 2.0$ that bound the region within which the model over- or underpredicts within a factor of two, along with lateral bars illustrating the calculated 95% confidence interval for MG .

3 VALIDATION CASES

3.1 Case summary

For an explosion simulator such as EXSIM, validation data could theoretically take the form of analytical solutions, experimental measurements or even information obtained from accidental events. Drawing from an extensive literature search, covering both open publications and DNV’s internal database, a library of validation cases was compiled for analysis. By design, the selected library of experimental works covers a broad range of parameters pertinent to explosion hazards, including congestion and confinement levels, ignition locations and fuel types.

A complete listing of the selected cases currently included in the EXSIM validation library is presented in Table 1.

Table 1: Summary of validation cases

Case ID	Description	Scale	Modelled Quantities	Num. Points <small>Note 1</small>	Ref(s).
1	SOLVEX	1:1, 1:6	Pressure	16	[4]
2	Troll Process Module	1:12	Pressure	2	[4]
3	CMI Offshore Modules (M24 and M25)	1:5	Pressure	15	[4]
4	DNV Module	1:1	Pressure	7	[4]
5	BFETS Phase 3a	1:1	Pressure	307	[14]
6	BFETS Phase 3b	1:1	Pressure	151	[17]
7	DNVGL Explosion Chamber	1:1	Pressure	35	[18]
8	HSL Repeated Pipe Congestion	1:1	Pressure	30	[19]
9	FM Global Vented Hydrogen Explosion Tests	1:1	Pressure	18	[20]
-	Overall	-	Pressure	581	-

Notes:

Note 1 – This corresponds to the total number of unique measurements used to assess the predictive capability of the model.

Brief summaries of the considered experimental programmes and the specific cases down-selected for modelling are provided in the following sections, along with overviews of the obtained results.

3.2 SOLVEX

3.2.1 Description and case selection

The SOLVEX (Shell Offshore Large Vented Explosions) experiments were performed by Shell in the early 1990s and the performance of an earlier version of EXSIM (EXSIM-94) against the resulting dataset was previously reported by Sæter [4].

The SOLVEX experiments considered pre-mixed methane and propane gas explosions within a vented, cuboidal enclosure at both full-scale and 1:6 scale (see Figure 3). The full-scale enclosure was 550 m³ in volume (with dimensions of 10.0 m x 8.8 m x 6.3 m) whilst its scaled counterpart had a volume of 2.5 m³ (with dimensions of 1.7 m x 1.5 m x 1.0 m).

Congestion levels within the enclosure were varied as required by adding or removing rows of vertical pipes. For both gas types, and at each scale, four different congestion levels were selected for analysis:

- No piping (empty enclosure)
- Rear row of piping only
- Front row of piping only
- Both front and rear rows of piping

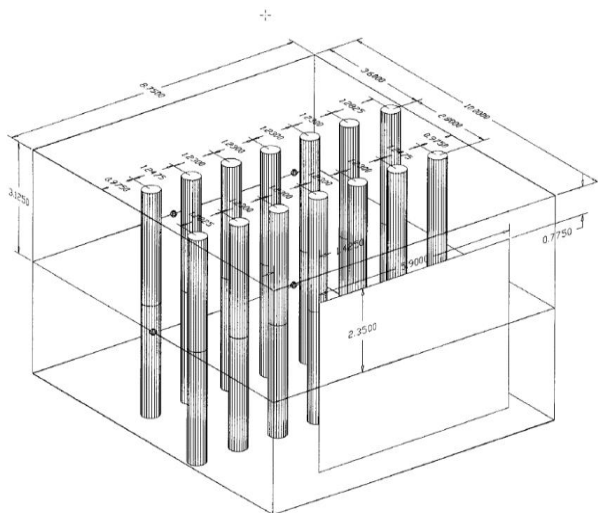


Figure 3: Illustration of full-scale SOLVEX enclosure

In all 16 cases, a single vent located at the front face of the enclosure (with a vent coefficient K_A , defined as the ratio of the area of the front face of the chamber and the area of the vent opening, of 0.5) was considered.

3.2.2 Model setup details

3.2.2.1 Geometry

Geometries for each configuration of interest at both 1:1 scale and 1:6 scale were constructed for use with EXSIM (i.e. the 'scaling factor' option with EXSIM was not used). A model snapshot showing the 3D model developed for the full-scale tests featuring both rows of piping is shown in Figure 4.

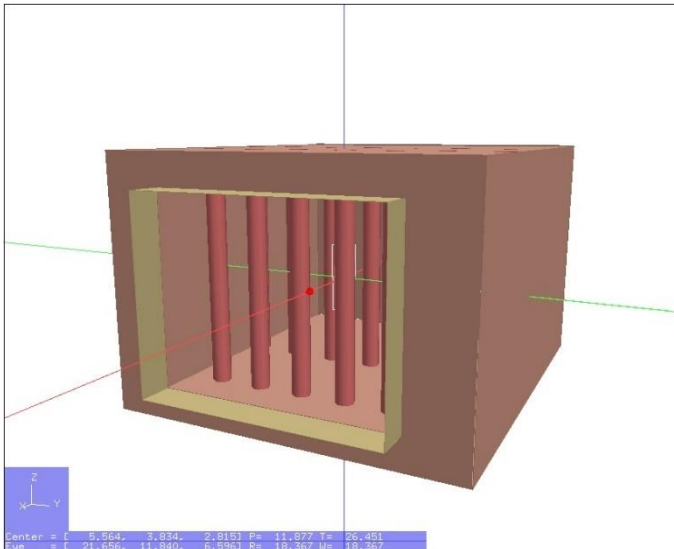


Figure 4: Example EXSIM 3D model for SOLVEX experiments

3.2.2.2 Gas composition

The fuel for each test was specified as pure methane or propane as appropriate. An equivalence ratio of 1.1, corresponding to slightly fuel-rich gas clouds, was utilised for all cases.

3.2.2.3 Fill fraction

In alignment with the experimental configuration, a 100% fill of the explosion chamber was defined within the model for all cases.

3.2.2.4 Ignition

A single ignition location, at the centre of the rear face of the chamber, was used for all cases.

3.2.2.5 Data monitoring

A total of four pressure monitors were placed within the enclosure (three floor-mounted, running from front to back, and a fourth on the rear wall) with a further two monitors positioned externally (one near the vent opening and another several metres beyond the front face of the enclosure).

The validation exercise considered measurements taken from the internally located transducers *exclusively*.

3.2.2.6 Computational mesh

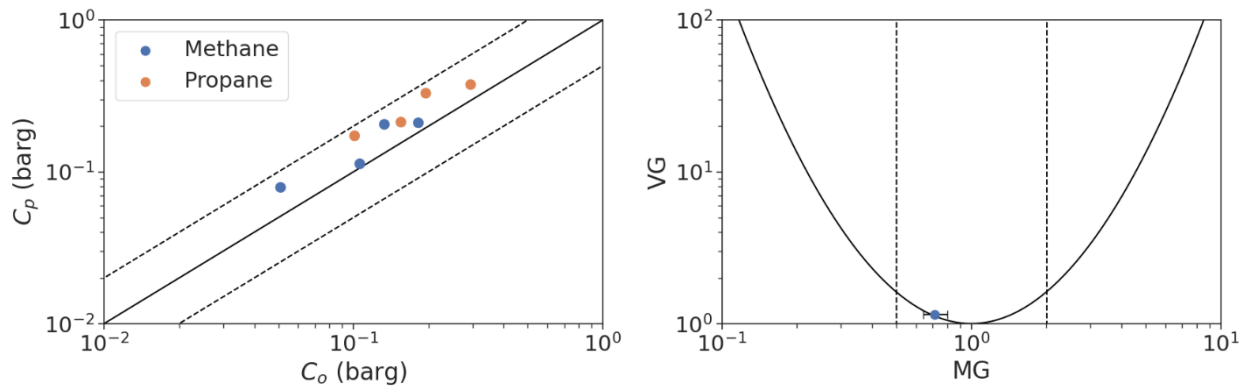
The mesh within the core combustion zone was defined as per the recommendations from EXSIMPOR. In all cases, this corresponded to cells of approximately 0.84 m in size. Beyond the region of interest, the cell size was allowed to grow with an expansion factor of 1.1.

3.2.2.7 Boundary conditions

The ground boundary (-z) was set to 'solid' for all cases, with all other boundaries set to 'open'.

3.2.3 Results

A summary of the 'max. of peak' pressure results obtained for the 1:1 scale tests are presented in Figure 5, whilst those obtained for the 1:6 scale tests are provided in Figure 6.

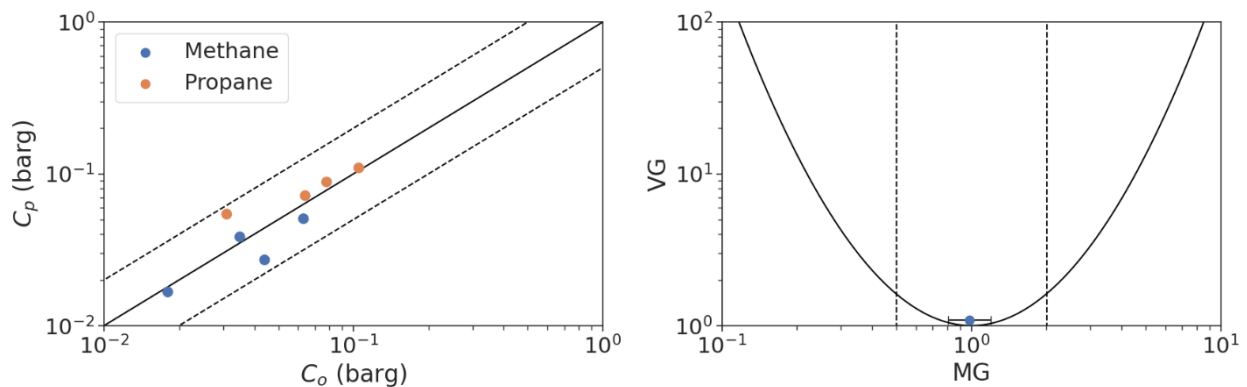


MG	95% CI ^{Note 1}	VG	FAC2
0.71	[0.64, 0.80]	1.15	1.00

Notes:

Note 1 – 95% confidence interval (CI) for MG

Figure 5: Validation results obtained for the modelled SOLVEX 1:1 cases



MG	95% CI ^{Note 1}	VG	FAC2
0.98	[0.81, 1.19]	1.08	1.00

Notes:

Note 1 – 95% confidence interval (CI) for MG

Figure 6: Validation results obtained for the modelled SOLVEX 1:6 cases

The following key observations were made based on the results obtained for the 1:1 scale and 1:6 scale SOLVEX tests:

- The code's predictions at both scales are generally very good, with the code typically tending towards overprediction. The exceptions were the 1:6 scale methane tests, for which a slight tendency to underpredict relative to the experimental values was observed.
- In all cases, the largest overpredictions were observed for the 'empty' configurations, where laminar combustion is dominant.



- The code predicts the correct trend as the geometry is altered, with the lowest peak pressures predicted for the 'empty' configurations and the largest peak pressures predicted for the most congested arrangements (i.e. two rows of piping).
- The code also predicts the correct trend as the fuel gas is altered, with the higher peak pressures obtained for the more reactive fuel gas (in this case, propane) in otherwise identical conditions.
- In all cases, the code's predictions were within a factor of 2 of the experimental values.

3.3 Troll Process Module

3.3.1 Description and case selection

These 1:12 scale gas explosion experiments were performed by Shell in the early 1990s and the performance of an earlier version of EXSIM (EXSIM-94) against a portion of the resulting dataset was previously reported by Sæter [4].

The overall experimental programme utilised 1:12 scale replicas of both a process module and a wellhead platform on Shell's Troll offshore platform. For the purposes of the validation exercise, only the process module tests (of which a total of 2 were performed) were considered.

The scaled process module rig had a volume of 4.8 m³ and a vent coefficient of 1.61 (with venting routes available via two sides of the module and the roof).

3.3.2 Model setup details

3.3.2.1 Geometry

A 1:12 scale 3D model of the Troll process module was constructed for use with EXSIM (i.e. the 'scaling factor' option with EXSIM was not used). A model snapshot showing the utilised 3D model is presented in Figure 7.

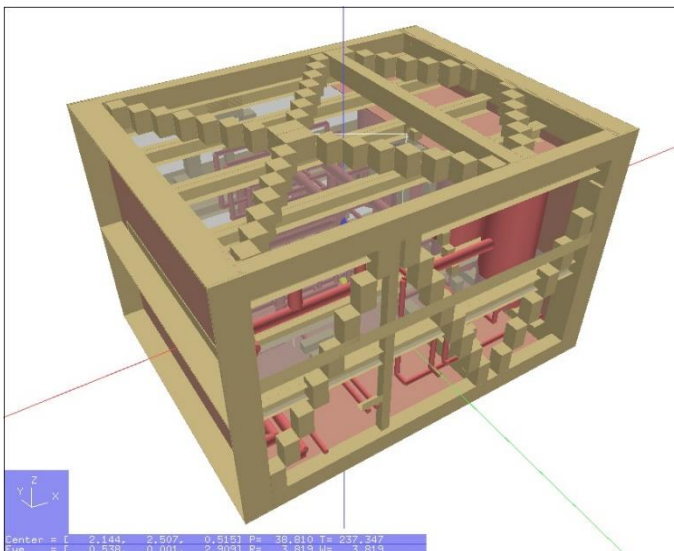


Figure 7: Example EXSIM 3D model

3.3.2.2 Gas composition

The fuel for each test was specified as pure propane. An equivalence ratio of 1.1, corresponding to slightly fuel-rich gas clouds, was utilised for all cases.

3.3.2.3 Fill fraction

In alignment with the experimental configuration, a 100% fill of the module was defined within the model for all cases.

3.3.2.4 Ignition

A total of two ignition locations were considered:

- One at the centre of the module; and
- One at the centre of the rear wall of the module.

3.3.2.5 Data monitoring

A total of five pressure monitors were defined within the enclosure: one in the centre of the module at floor level and a further two mounted at intermediate heights on each of the opposing walls.

3.3.2.6 Computational mesh

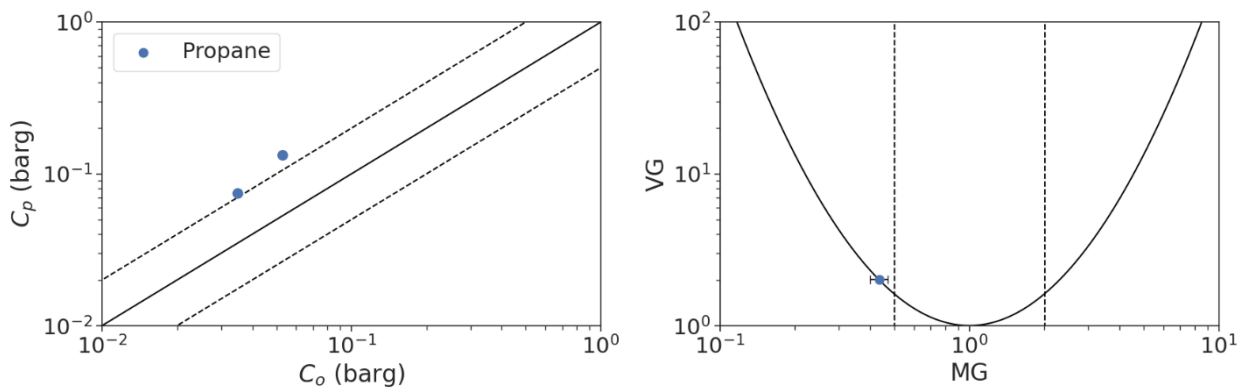
The mesh within the core combustion zone was defined as per the recommendations from EXSIMPOR. In all cases, this corresponded to cells of approximately 0.17 m in size. Beyond the region of interest, the cell size was allowed to grow with an expansion factor of 1.05.

3.3.2.7 Boundary conditions

The ground boundary (-z) was set to 'solid' for all cases, with all other boundaries set to 'open'.

3.3.3 Results

A summary of the 'max. of peak' pressure results obtained for the Troll process module are presented in Figure 8.



MG	95% CI ^{Note 1}	VG	FAC2
0.43	[0.40, 0.47]	2.02	0.00

Notes:

Note 1 – 95% confidence interval (CI) for MG

Figure 8: Validation results obtained for the modelled Troll Process Module cases

The following key observations were made based on the results obtained for the 1:12 scale Troll process module tests:

- Whilst it is recognised that the available data for comparison are limited in number, the code shows a clear tendency to overpredict for this case.
- The code predicts the expected trend as the ignition location is altered, with 'edge' ignition yielding higher peak pressures than 'centre' ignition.
- In both cases, the code's overpredicted by more than a factor of 2 relative to the experimentally obtained values.

3.4 CMI Offshore Compressor (M24) and Separator (M25) Modules

3.4.1 Description and case selection

This experimental programme was performed by the Christian Michelson Institute (CMI) and the performance of an earlier version of EXSIM (EXSIM-94) against the resulting dataset was previously reported by Sæter [4].

The overall experimental programme assessed flame and pressure development inside representative offshore modules at scales of 1:5 and 1:33. At each scale, two different layouts (representative of realistic compressor and separator modules) were tested, along with up to six distinct venting configurations (vent parameter ranging from 0.92 to 4.78) and up to four ignition locations (either centrally on the upper or lower decks, or at the north ends of the modules on the upper or lower decks). All tests were performed with stoichiometric methane-air or propane-air gas mixtures.

For the purposes of the validation exercise, a representative set of 15 unique experiments from the 1:5 scale test series were selected for assessment, as shown in Table 2. The selected tests cover a range of layouts, ignition locations and venting configurations (note that consideration of different venting configurations was limited to the separator module).

Table 2: Summary of selected cases for modelling

Simulation ID	Module	Fuel	Ignition Location	Vent Parameter	Notes
1	Compressor (M24)	Methane	Lower Deck, Central	0.92	-
2	Compressor (M24)	Propane	Lower Deck, Central	0.92	-
3	Compressor (M24)	Methane	Upper Deck, Central	0.92	-
4	Compressor (M24)	Propane	Upper Deck, Central	0.92	-
5	Compressor (M24)	Methane	Lower Deck, North End	0.92	-
6	Separator (M25)	Methane	Lower Deck, Central	0.92	-
7	Separator (M25)	Methane	Upper Deck, Central	0.92	-
8	Separator (M25)	Propane	Upper Deck, Central	0.92	-
9	Separator (M25)	Methane	Upper Deck, Central	0.46	-
10	Separator (M25)	Methane	Upper Deck, Central	1.42	-
11	Separator (M25)	Methane	Upper Deck, Central	1.98	-

Simulation ID	Module	Fuel	Ignition Location	Vent Parameter	Notes
12	Separator (M25)	Methane	Upper Deck, Central	2.85	-
13	Separator (M25)	Methane	Upper Deck, Central	4.78	-
14	Separator (M25)	Methane	Upper Deck, Central	0.92	'Empty module' case
15	Separator (M25)	Propane	Upper Deck, Central	0.92	'Empty module' case

3.4.2 Model setup details

3.4.2.1 Geometry

Geometries for the two modules were constructed for each required venting configuration at full scale, and subsequently scaled down by a factor of 5 using EXSIM's 'scaling' option to yield the required 1:5 scale geometries. Model snapshots showing examples of the 3D models developed for the compressor and separator modules are presented in Figure 9.

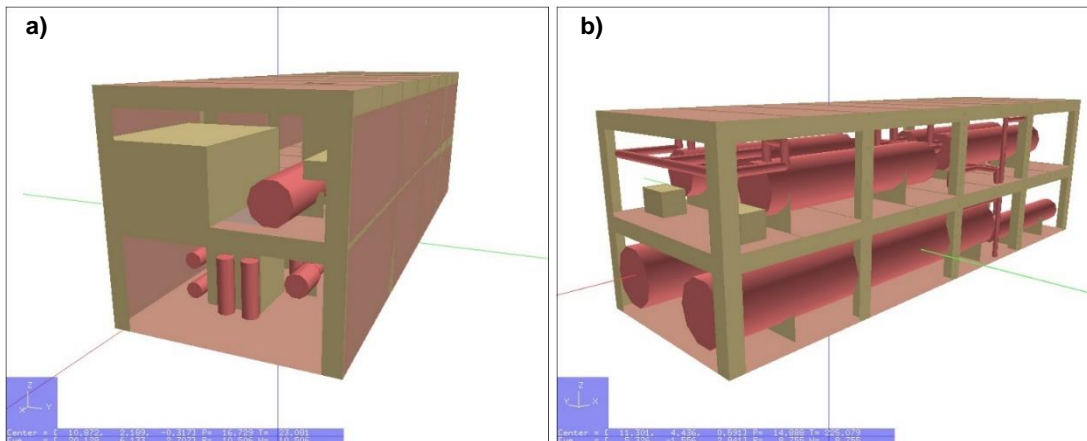


Figure 9: EXSIM 3D model for the a) Compressor Module (vent parameter = 0.92) and b) Separator Module (vent parameter = 4.78)

3.4.2.2 Gas composition

The fuel for each test was specified as pure methane or propane as appropriate. An equivalence ratio of 1.0, corresponding to stoichiometric gas clouds, was utilised for all cases.

3.4.2.3 Fill fraction

In alignment with the experimental configurations, a 100% module fill was defined within the model for all cases.

3.4.2.4 Ignition

For each test, point ignition at either the deck centre or north end of each deck level was specified as required.

3.4.2.5 Data monitoring

Five pressure monitors were defined within the enclosure:

- Two on the upper deck, attached to the underside of the enclosure roof (in the middle and the other at one end);
- A further three on the lower deck (one at each end and a third halfway between them).

3.4.2.6 Computational mesh

The mesh within the core combustion zone for each module was defined as per the recommendations from EXSIMPOR. In all cases, this corresponded to cells of approximately 1.84 m in size. Beyond the region of interest, the cell size was allowed to grow with an expansion factor of 1.05.

3.4.2.7 Boundary conditions

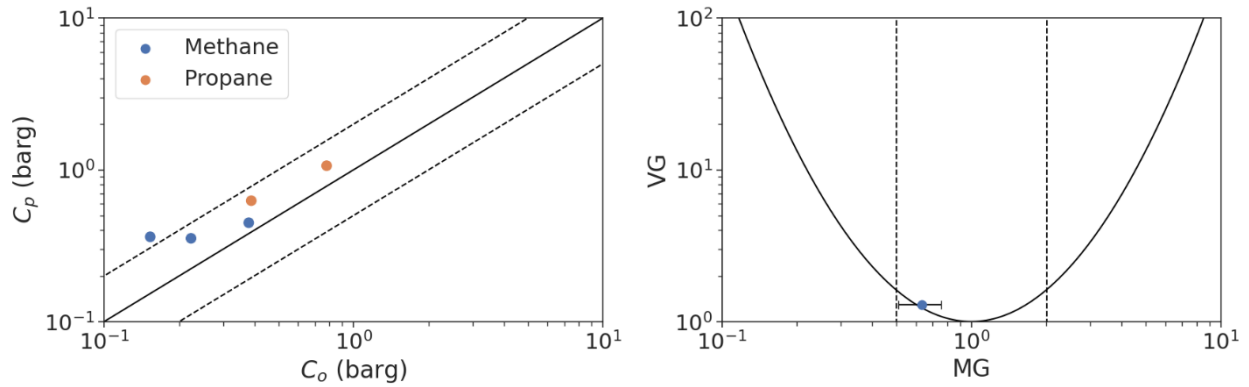
The ground boundary (-z) was set to 'solid' for all cases, with all other boundaries set to 'open'.

3.4.3 Results

Summaries of the 'max. of peak' pressure results obtained for the 1:5 scale Compressor Module (M24) and Separator Module (M25) tests are presented in Figure 10 and Figure 11, respectively.

The following key observations were made based on the results of the 1:5 scale compressor and separator module tests:

- The initial results for the compressor module cases, which considered variations in ignition location and fuel type only, indicated that the code's predictions are in good agreement with the experimental data, albeit with a slight tendency to overpredict (especially at lower pressures).
- For the compressor module, the code was able to predict overpressures to within a factor of 2 of the experimental values in 80% of the considered cases.
- For the separator module cases, which considered variations in venting arrangement along with ignition location and fuel type, there is greater scatter than observed for the compressor module cases, with a much stronger tendency to overpredict at lower pressures. The primary contributor to the observed scatter was identified to be the large overprediction made for the 'empty' module cases (see below).
- Despite the scatter, the code correctly captured the observed trends as the levels of congestion and confinement were modified, predicting higher pressures for more congested and/or confined geometries.
- For the separator module, the code was able to predict overpressures to within a factor of 2 of the experimental values in 40% of the considered cases. The largest overpredictions were observed for the 'empty' module cases, where the experimental peak pressure was overpredicted by a factor of approximately 4.
- For both modules, EXSIM predicted the correct trends as the fuel gas was altered, with higher peak pressures obtained for more reactive fuel gases in otherwise identical conditions.

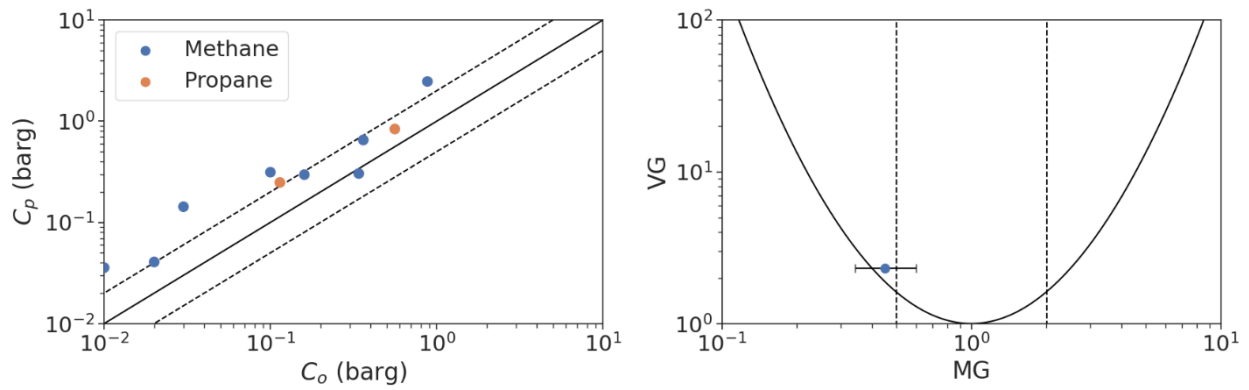


MG	95% CI ^{Note 1}	VG	FAC2
0.64	[0.51, 0.76]	1.30	0.80

Notes:

Note 1 – 95% confidence interval (CI) for MG

Figure 10: Validation results obtained for the modelled 1:5 scale CMI Compressor Module (M24) cases



MG	95% CI ^{Note 1}	VG	FAC2
0.45	[0.34, 0.60]	2.33	0.40

Notes:

Note 1 – 95% confidence interval (CI) for MG

Figure 11: Validation results obtained for the modelled 1:5 scale CMI Separator Module (M25) cases

3.5 DNV Module

3.5.1 Description and case selection

This set of experiments was performed by DNV and the performance of an earlier version of EXSIM (EXSIM-94) against the resulting dataset was previously reported by Sæter [4].

The tests assessed pressure development arising from ignition of rich propane-air clouds within a vented, 35 m³ cuboidal enclosure. Congestion levels within the enclosure were adjusted via mounting up to 4 rows of horizontal pipes or boards in various configurations.

Venting for each configuration was provided via a floor-mounted orifice on the front face of the enclosure, with up to two orifice sizes (corresponding to vent parameters of 0.33 and 0.82) considered for each configuration. For all tests, the enclosure was filled with a rich propane-air gas mixture (equivalence ratio of 1.3) with an ignition point located at the centre of the rear wall.

From the overall experimental campaign, 7 tests were selected for assessment – see Table 3. The selected tests cover a range of congestion levels (and obstacle shapes) and venting configurations.

Table 3: Summary of selected cases for modelling

Experiment ID	Obstacle Type	Vent Parameter	Notes
veri1	Boards	0.82	4 rows of boards, Full venting
veri2	Pipes	0.82	4 rows of pipes, Full venting
veri3	Pipes	0.82	2 rows of pipes, Full venting
veri4	Pipes	0.82	1 row of pipes, Full venting
veri5	None (Empty)	0.82	Empty enclosure, Full venting
veri6	Pipes	0.33	1 rows of pipes, Reduced venting
veri8	Boards	0.82	1 row of boards, Full venting

3.5.2 Model setup details

3.5.2.1 Geometry

The DNV enclosure is cuboidal, with dimensions 4.0 m x 2.5 m x 3.6 m. Two venting configurations at the front face of the enclosure are considered: full venting (i.e. the front face of the enclosure is fully open) and partial venting (where the face of the enclosure is blocked by a full size plate with a full width cut-out extending from ground level up to a height of 1.44 m).

A full-scale 3D model of the enclosure was constructed for each congestion/venting configuration of interest. A model snapshot showing the utilised 3D model is presented in Figure 12.

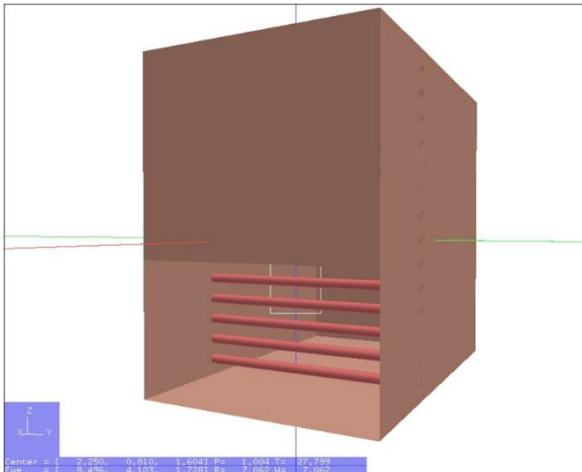


Figure 12: Example EXSIM 3D model of the DNV enclosure (vent parameter = 0.33)

3.5.2.2 Gas composition

The fuel for each test was specified as propane, with an equivalence ratio of 1.3.

3.5.2.3 Fill fraction

In alignment with the experimental configurations, a 100% fill of the enclosure was defined within the model for all cases.

3.5.2.4 Ignition

For each test, point ignition at the centre of the rear wall (i.e. the wall opposite the vent) was specified.

3.5.2.5 Data monitoring

A total of four pressure monitors were defined within the enclosure: one mounted centrally and a further three at the face-centres of the floor, ceiling and one of the sidewalls). A fifth monitor was located near the vent opening, with two others located at increasing distances beyond the front face of the enclosure.

The validation exercise considered measurements taken from the internally located transducers *exclusively*.

3.5.2.6 Computational mesh

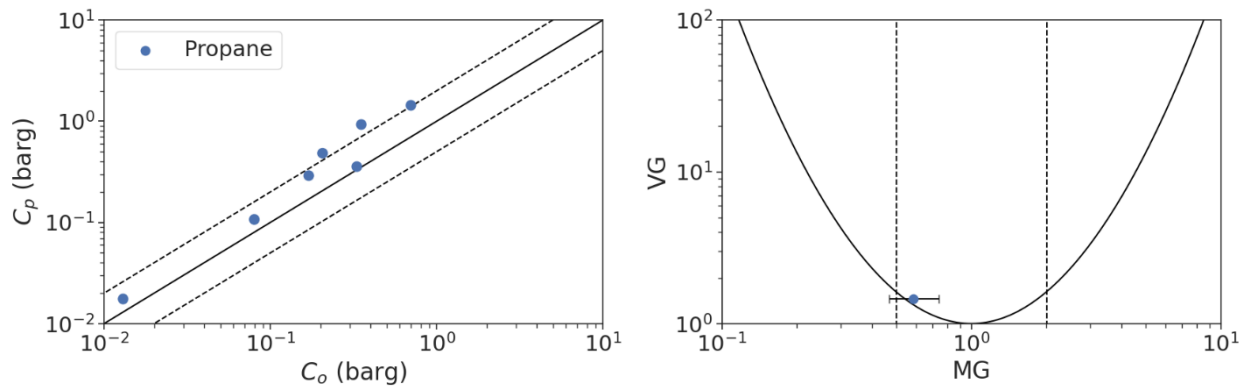
The mesh within the core combustion zone was defined as per the recommendations from EXSIMPOR. In all cases, this corresponded to cells of approximately 0.38 m in size. Beyond the region of interest, the cell size was allowed to grow with an expansion factor of 1.1.

3.5.2.7 Boundary conditions

The ground boundary (-z) was set to 'solid' for all cases, with all other boundaries set to 'open'.

3.5.3 Results

A summary of the 'max. of peak' pressure results obtained for the modelled tests is presented in Figure 13.



MG	95% CI ^{Note 1}	VG	FAC2
0.59	[0.47, 0.74]	1.46	0.57

Notes:

Note 1 – 95% confidence interval (CI) for MG

Figure 13: Validation results obtained for the modelled DNV Module cases

The following key observations were made based on the results obtained for the modelled DNV Module cases:

- EXSIM's predictions for the modelled cases can be seen to be generally good, with a tendency to overpredict relative to the experimentally obtained values.
- The trends of the predicted and measured overpressures were found to be in close agreement, with rows of boards yielding larger overpressures than their piping-based equivalents and peak pressures increasing as the vent area is reduced.
- Overall, 57% of the EXSIM predictions were assessed to be within a factor of 2 of the experimental result.

3.6 BFETS Phase 3A

3.6.1 Description and case selection

These full-scale gas explosion experiments were performed as part of the Blast and Fire Engineering Project for Topside Structures (BFETS) joint industry project, which was originally kicked-off in 1990. The Phase 3A experiments considered here were performed between May 1997 and March 1998 [14].

As per the other project phases, the Phase 3A test programme involved full-scale experiments in a test rig designed to approximate the layout of a typical offshore module, with dimensions 28 m x 12 m x 8 m (see Figure 14). In addition to considering a range of equipment layouts (O1 to O5), degrees of confinement (C1 to C3 – see Figure 14) and ignition locations (I1 to I4), the programme also evaluated the impact of deluge on the generated overpressures. The majority of the experiments used near-stoichiometric mixtures of natural gas (~90% methane) and air, whilst a limited number used propane.

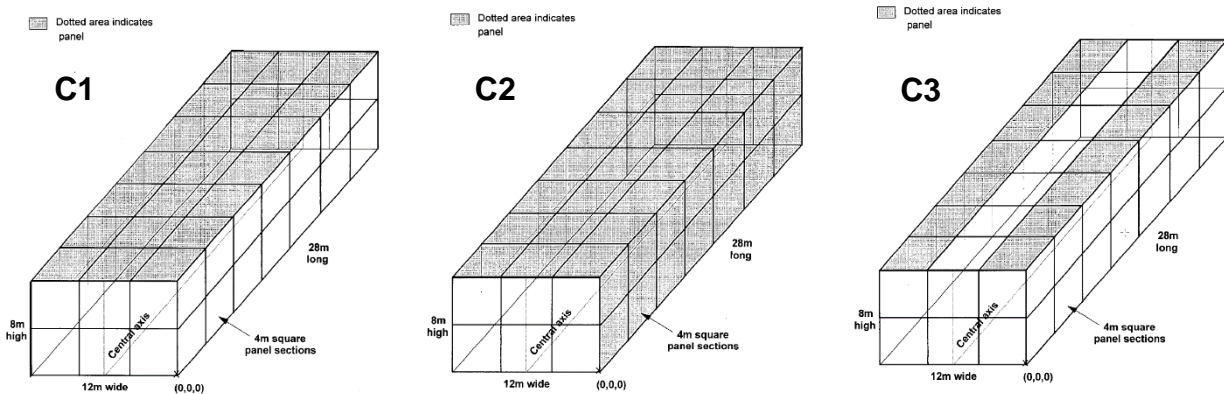


Figure 14: Views of test rig (upper pane) and assessed confinement configurations (lower panes) [14]

For the purposes of the validation exercise, a representative set of 10 experiments was selected for assessment, as shown in Table 4. The selected tests were based on Layout O1 and cover a range of ignition locations and venting/confinement configurations. It should be noted that, for ease of reference, the quoted test numbers correspond to those used in Table 4.3 within the original report.

Table 4: Summary of selected cases for modelling ^{Note 1}

Test No.	Equipment Layout	Confinement Configuration	Ignition Position	Water Deluge
1	O1	C1	I1	None
2	O1	C1	I2	None
3	O1	C1	I4	None
4	O1	C1	I3	None
8	O1	C2	I2	None
9	O1	C2	I4	None
16	O1	C3	I2	None
17	O1	C3	I4	None
19	O1	C3	I3	None
22 ^{Note 2}	O1	C3	I3	None

Notes:

Note 1– Test 18 was excluded due to uncertainties relating to the ignition location (see Ref. [14] for details).

Note 2– Repeat of Test 19.

3.6.2 Model setup details

3.6.2.1 Geometry

The baseline geometry was created by directly importing a detailed 3D model of the test rig into EXSIM (shown in Figure 15). The geometry was then adjusted manually as necessary to produce the required confinement configurations.



Figure 15: Example EXSIM 3D model of the test rig (confinement configuration = C1)

3.6.2.2 Gas composition

As none of propane tests involved Equipment Layout O1, the selected tests included natural gas-air mixtures exclusively. The report lists some representative compositions for the utilised natural gas – all typically involved 90-92% methane (see Table 5, below).

Table 5: Summary of measured natural gas compositions (Ref. [14], Table 4.1)

Test No.	Component - % of Sample (v/v)							
	CH ₄	C ₂ H ₆	C ₃ H ₈	C ₄ H ₁₀	C ₅ +	N ₂	O ₂	C ₂ H ₄
1-11	90.82	8.02	0.88	0.21	0.03	0.04	0.00	0.00
12-23	90.74	7.97	0.97	0.23	0.04	0.05	0.00	0.00
24-34	90.08	8.35	1.18	0.27	0.06	0.07	0.00	0.00
35-45	91.74	7.06	0.94	0.18	0.03	0.05	0.00	0.00

Due to the lack of variation in composition across the various samples, the composition from Test Number HSE01-HSE11 (90.82% Methane) was selected for use in all simulations.

As EXSIM has only a limited number of selectable gases, it was necessary to define a ‘pseudo gas’ to represent the required natural gas composition (note: for such cases, EXSIM effectively creates a blend of methane and propane for the specified molecular weight).

For the selected composition, a molecular weight of 18.9 g/mol was calculated and input into the model. Equivalence ratios for each case were specified as per Ref. [14].

3.6.2.3 Fill fraction

In alignment with the experimental configuration, a 100% fill of the test rig was defined within the model for all cases.

3.6.2.4 Ignition

The four ignition locations (I1-I4) are provided in Table 3.6 of Ref. [14]. Ignition locations I1 and I2 were located centrally within the module at elevations of 0.4 m (I1) and 5.0 m (I2). Locations I3 and I4 provided edge and corner ignitions at elevation of 2.0 m and 0.4 m, respectively

3.6.2.5 Data monitoring

The test rig (and the surrounding area) was fitted with a large number of pressure transducers, with the locations varying to some degree between tests. The various coordinates were entered into the code as required.

Due to the large number of monitors, the details are not repeated here. However, the coordinates can be found in Table 3.7(a) (and subsequent tables) within the original report. It should be noted that the validation exercise considered measurements taken from the internally located transducers *exclusively*.

3.6.2.6 Computational mesh

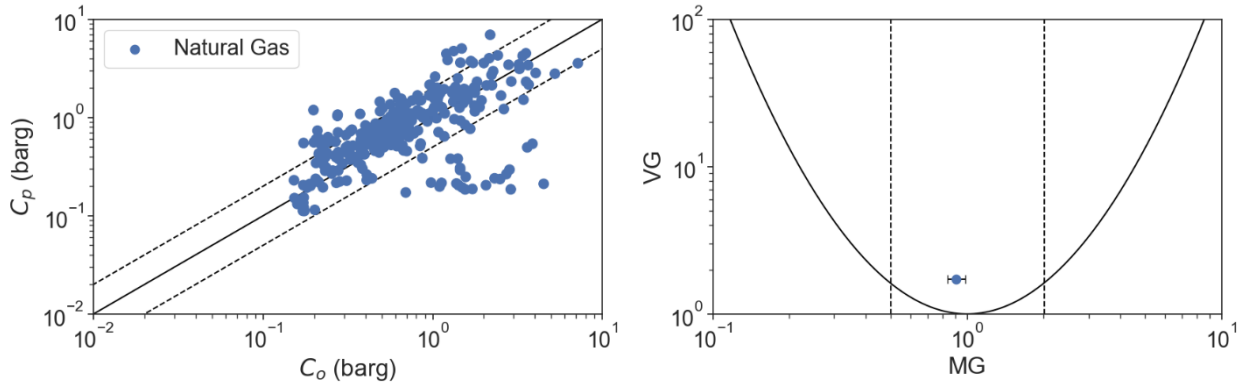
In all cases, the cell size within the core combustion zone (within the test rig) was set based on the recommendation provided by EXSIMPOR. Beyond the region of interest, the cell size was allowed to grow with an expansion factor of 1.1.

3.6.2.7 Boundary conditions

The ground boundary (-z) was set to ‘solid’ for all cases, with all other boundaries set to ‘open’.

3.6.3 Results

A summary of the results obtained for direct point-by-point 'peak pressure' comparisons of the modelled BFETS 3a cases are presented in Figure 16, below. Comparisons between experimental observation and model prediction via the 'max. of peak' measure (see Section 2.4) are provided in Figure 17.

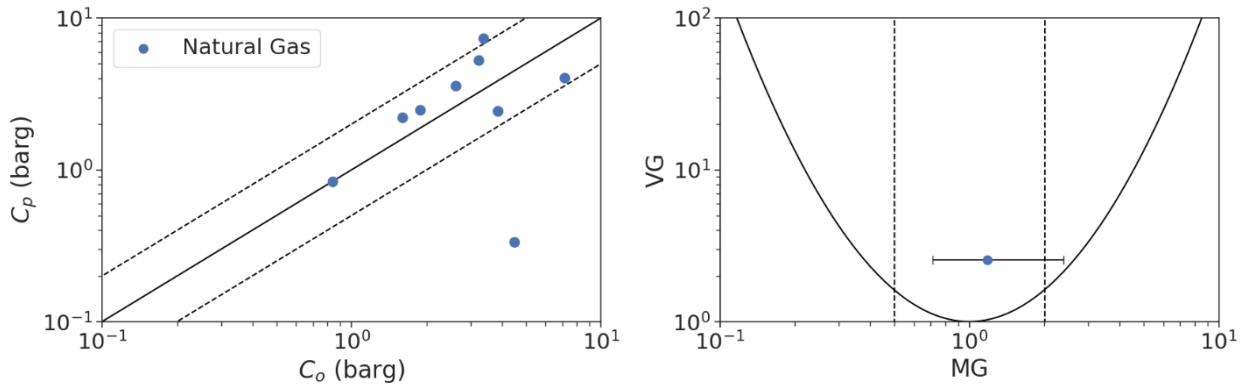


MG	95% CI ^{Note 1}	VG	FAC2
0.91	[0.84, 1.00]	1.76	0.77

Notes:

Note 1 – 95% confidence interval (CI) for MG

Figure 16: Validation results obtained for modelled BFETS Phase 3A Cases (direct point-by-point comparison)



MG	95% CI ^{Note 1}	VG	FAC2
1.18	[0.71, 2.38]	2.55	0.78

Notes:

Note 1 – 95% confidence interval (CI) for MG

Figure 17: Validation results obtained for modelled BFETS Phase 3A Cases ('max. of peak' comparison)

The following key observations were made based on the results obtained for the modelled BFETS Phase 3A cases:

- Considering first the direct point-by-point comparison results (where results from individual pressure transducers are directly compared against the model's predictions), it can be seen that the code generally performs very well, tending towards overprediction at all pressure levels. In this case, the code's predictions were found to lie within a factor of two of the experimental values 77% of the time.
- For the 'max. of peak' measure, the code's predictions can be seen to compare very favourably with experiment, showing a slight tendency towards overprediction. Here, the code's predictions were found to lie within a factor of two of the experimental values 78% of the time.
- The code also predicts the correct trends as the level of confinement and ignition location is varied, with higher pressures obtained for higher degrees of confinement and for edge/corner ignition locations.

When considering the above, it should be noted that the reproducibility of the closely related Phase 3B experiments was found to be limited, highlighting the natural limit imposed on the accuracy that can be achieved with explosion models (the peak pressures recorded in the nominally identical Phase 3A Tests 19 and 22 varied by up to a factor of 1.6, for example) – further details may be found in Ref. [15]. Subsequent work by Hansen et al. [16] suggested that the poor reproducibility may, in part, be due to the occurrence of detonations within the full-scale rig – this, in turn, may account for some of the underpredictions observed at higher pressure levels, as EXSIM is not designed to model DDT events.

3.7 BFETS Phase 3B (full scale tests)

3.7.1 Description and case selection

These full-scale gas explosion experiments were performed as part of the Blast and Fire Engineering Project for Topside Structures (BFETS) joint industry project and followed-on from the Phase 3A experiments discussed in Section 3.6 [17].

The primary aim of the full-scale Phase 3B tests was to investigate the explosions loads generated in more realistic conditions those considered in their Phase 3A counterparts, which were based on homogenous, (near) stoichiometric gas clouds that flooded the entire test rig. To this end, a series of full scale explosions tests were performed for gas clouds occupying only part of the rig.

The Phase 3B experiments were based on the same full-scale test rig as their Phase 3A counterparts, but were limited to a single equipment layout (Layout O1), confinement configuration (see Figure 18), fuel type (natural gas) and ignition location (Location I1). The test series comprised five partial fill experiments and a single 'full fill' base case setup – all six tests were modelled in EXSIM.

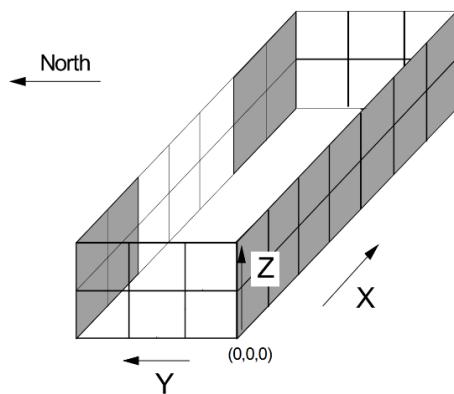


Figure 18: Assessed confinement configuration for Phase 3B tests (rig roof not shown for clarity) [17]

3.7.2 Model setup details

3.7.2.1 Geometry

The 3D geometry required for the analysis was constructed by adjusting one of the previously developed Phase 3A geometries (see Section 3.6.2.1) to reflect the required confinement arrangement. The resulting EXSIM geometry, which was used for all six tests in the series, is shown in Figure 19.

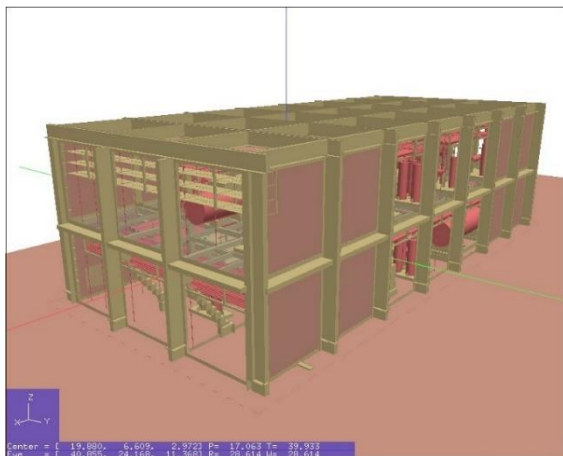


Figure 19: EXSIM 3D model for BFETS Phase 3B tests

3.7.2.2 Gas composition

In alignment with the Phase 3A tests, a pseudo gas with a molecular weight of 18.9 g/mol was used in support of the analysis for all six tests. An equivalence ratio of 1.0 was applied for all tests to reflect the 'nominally stoichiometric' fuel-air mixtures used in the experiments.

3.7.2.3 Fill fraction

The test programme consisted of five partial fill arrangements and a single 'full fill' set up, as summarised in Table 6 and Figure 20.

Table 6: Summary of modelled cloud sizes

Test No.	Cloud Dimensions (m)			Rig Fill Fraction
	X	Y	Z	
1	8	8	8	19%
2	4	8	8	10%
3	12	12	8	43%
4	12	12	8	43%
5	28	12	8	100%
6	8	8	8	19%

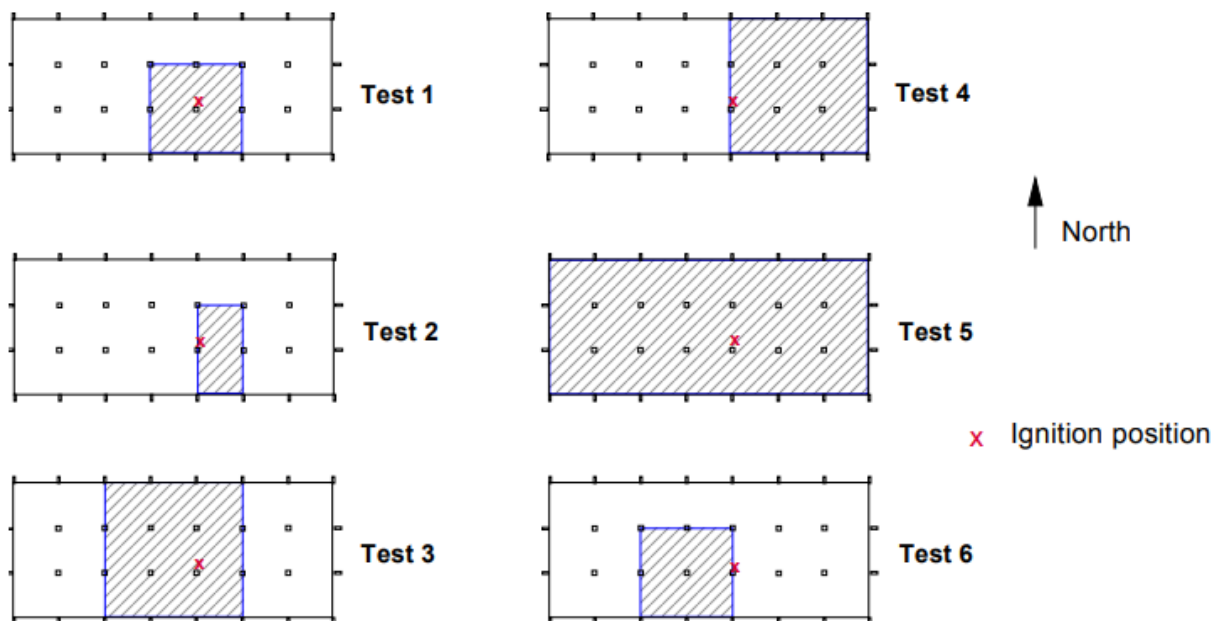


Figure 20: View of modelled cloud configurations

3.7.2.4 Ignition

A single, approximately centrally located, ignition point was used for all tests (as shown in Figure 21).

3.7.2.5 Data monitoring

The test rig (and the surrounding area) was fitted with a large number of pressure transducers. The various coordinates were entered into the code as required.

Due to the large number of monitors, the details are not repeated here. However, the coordinates can be found in Table 2a (and subsequent tables) within the original report. It should be noted that the validation exercise considered measurements taken from the internally located transducers *exclusively*.

3.7.2.6 Computational mesh

In all cases, the cell size required within the core combustion zone was set based on the recommendation provided by EXSIMPOR. The recommended cell size for each case, which ranged from 0.54 m to 0.63 m, was then uniformly applied throughout the test rig.

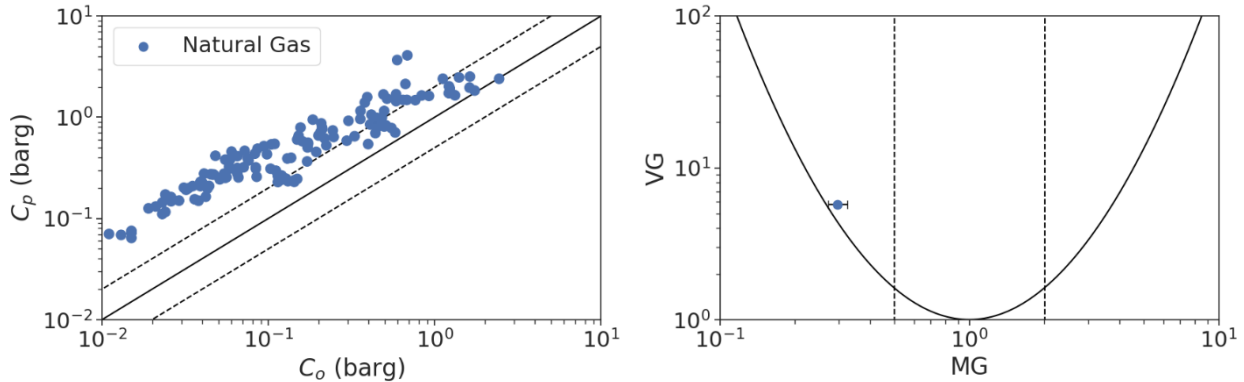
Beyond the region of interest, the cell size was allowed to grow with an expansion factor of 1.05.

3.7.2.7 Boundary conditions

The ground boundary (-z) was set to 'solid' for all cases, with all other boundaries set to 'open'.

3.7.3 Results

A summary of the results obtained for direct point-by-point 'peak pressure' comparisons of the modelled BFETS 3B cases are presented in Figure 21, below. Comparisons between experimental observation and model prediction via the 'max. of peak' measure (see Section 2.4) are provided in Figure 22.

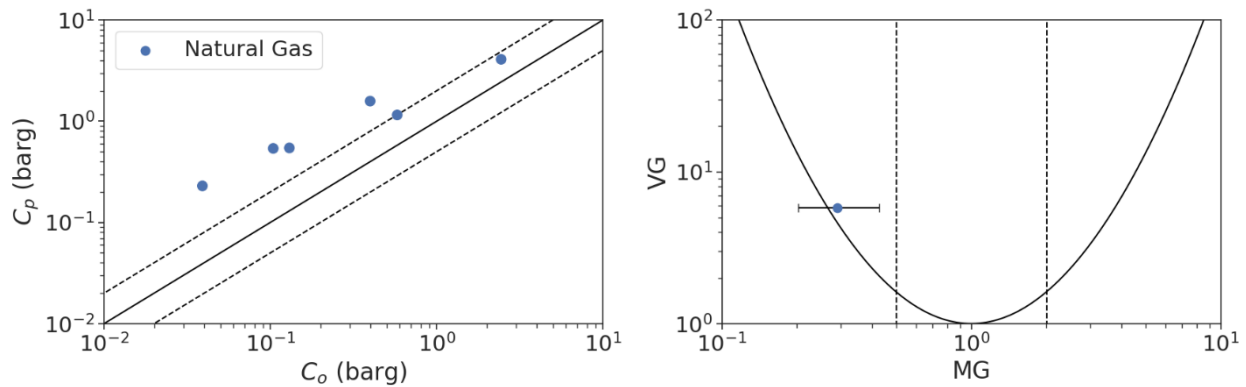


MG	95% CI ^{Note 1}	VG	FAC2
0.30	[0.27, 0.32]	5.71	0.20

Notes:

Note 1 – 95% confidence interval (CI) for MG

Figure 21: Validation results obtained for modelled BFETS Phase 3B cases (direct point-by-point comparison)



MG	95% CI ^{Note 1}	VG	FAC2
0.29	[0.20, 0.43]	5.80	0.33

Notes:

Note 1 – 95% confidence interval (CI) for MG

Figure 22: Validation results obtained for modelled BFETS Phase 3B cases ('max. of peak' comparison)

The following key observations were made based on the results obtained for the modelled BFETS Phase 3B cases:

- Both the direct point-by-point and 'max. of peak' measures show that code tends to overpredict for smaller cloud sizes (and, by extension) at lower pressure levels, with the prediction quality increasing for larger clouds and more damaging overpressures.
- For the direct point-by-point comparison, the code's predictions were found to lie within a factor of two of the experimental result 20% of time. An equivalent value of 33% was obtained for the 'max. of peak' measure.
- The code predicts the correct trends as the cloud size is varied, with higher pressures obtained for larger cloud sizes (for similar congestion levels).

When considering the above, it should be noted that the reproducibility of the Phase 3B experiments was found to be limited, highlighting the natural limit imposed on the accuracy that can be achieved with explosion models – further details may be found in Ref. [17].

3.8 DNVGL Explosion Chamber

3.8.1 Description and case selection

This series of experiments was performed at the Spadeadam test site with a view to assessing the impact of congestion levels and vent size on confined gas explosions [18]. A total of 38 tests were performed for stoichiometric natural gas mixtures within a vented, 182 m³ explosion chamber (see Figure 23).



Figure 23: DNVGL explosion chamber

Congestion levels within the chamber were adjusted via mounting arrays of horizontal pipes in various configurations, with the overall volume blockage varying between 0% and 5%. Each configuration was assessed for up to four distinct vent sizes (varied by adjusting the opening at the front face of the chamber): 20.25 m² (fully open), 10.13 m² (50% open), 5.06 m² (25% open) and 2.25 m² (11% open).

All 38 tests were modelled in EXSIM.

3.8.2 Model setup details

3.8.2.1 Geometry

Geometries for each of the 38 tests were manually constructed for use with EXSIM. An example model snapshot is shown in Figure 24.

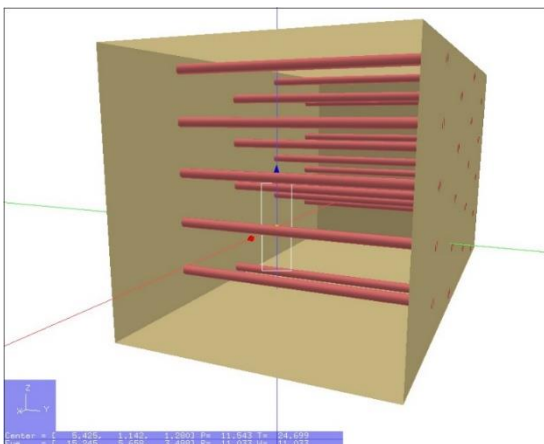


Figure 24: Example EXSIM 3D model of the DNVGL explosion chamber

3.8.2.2 Gas composition

Whilst the reference paper stated that all tests were performed for a stoichiometric natural gas mixture, detailed composition data was not provided. Accordingly, the make-up of the gas mixture was approximated as methane-air with an equivalence ratio of 1.05 for all cases.

3.8.2.3 Fill fraction

In alignment with the experimental configuration, a 100% fill of the explosion chamber was defined within the model for all cases.

3.8.2.4 Ignition

A single ignition location, at the centre of the rear face of the chamber, was used for all 38 tests.

3.8.2.5 Data monitoring

The explosion chamber was fitted with 5 pressure transducers (attached to the floor); a further 3 transducers, mounted 1.5 m above ground level, were positioned externally.

The validation exercise considered measurements taken from the internally located transducers *exclusively*.

3.8.2.6 Computational mesh

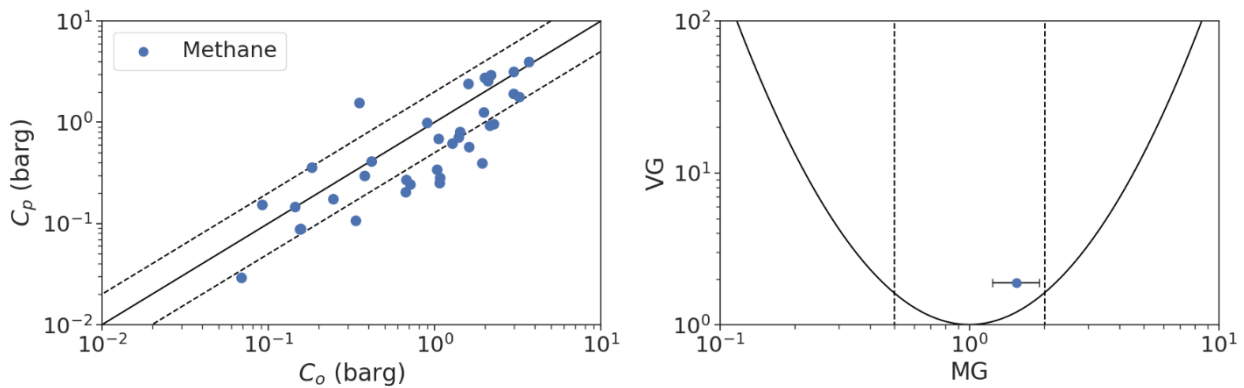
The mesh within the core combustion zone for each module was defined as per the recommendations from EXSIMPOR. In all cases, this corresponded to cells of approximately 0.57 m in size. Beyond the region of interest, the cell size was allowed to grow with an expansion factor of 1.05.

3.8.2.7 Boundary conditions

The ground boundary (-z) was set to 'solid' for all cases, with all other boundaries set to 'open'.

3.8.3 Results

A summary of the 'max. of peak' pressure results obtained for the DNVGL Explosion Chamber test series are presented in Figure 25, below.



MG	95% CI ^{Note 1}	VG	FAC2
1.54	[1.23, 1.91]	1.89	0.60

Notes:

Note 1 – 95% confidence interval (CI) for MG

Figure 25: Validation results obtained for modelled DNVGL explosion chamber cases

The following key observations were made based on the provisional results:

- The initial results indicate that the code, overall, performs well for this test, albeit with a tendency to underpredict.
- The code correctly captured the observed trends as the levels of congestion and confinement were modified, predicting higher pressures for more congested and/or confined geometries.
- Across the complete set of 38 cases, EXSIM was found, overall, to underpredict the peak pressures (albeit within a factor of two). Some contribution to the observed underprediction is likely to originate from the approximation of the fuel gas (natural gas) by a less reactive gas (methane) – a coarse sensitivity test using a ‘typical’ natural gas composition indicated that peak pressures could be boosted by approximately 10% if such a refinement is made.
- Some variation in prediction accuracy was observed as a function of vent size. To a degree, this variation is attributable to the selected computational mesh, which limited the accuracy with which the available vent area could be modelled (leading to excessive or insufficient venting of the developing explosion).

3.9 Shell/HSL hydrogen repeated pipe congestion

3.9.1 Description and case selection

This series of experiments was performed at the UK Health and Safety Laboratory (HSL) test site with the aim of gaining a better understanding of the potential consequences of hydrogen explosions in congested environments [19].

The test series was based on ignition of hydrogen-air mixtures within a modular test rig of dimensions 3 m (length) x 3 m (width) x 2 m (height), as shown in Figure 26.



Figure 26: Shell/HSL hydrogen repeated pipe congestion test rig (4-gate configuration) [19]

For each test, congestion within the rig was set to one of three levels (referred to as '4-gate', '7-gate' and '9-gate') via adding/removing grids of 125 mm steel bars in concentric square patterns around a fixed central ignition point. Five distinct hydrogen-air stoichiometries were assessed for the 4-gate configuration, (ranging from 0.97 to 1.71), whilst only a single stoichiometry was assessed for each of the 7-gate and 9-gate arrangements (1.17 and 1.28, respectively).

The 4-gate and 7-gate tests were all unconfined, whereas a single confining wall (positioned 1.7 m from the rig boundary) was introduced for the 9-gate case.

From the overall experimental campaign, the 4-gate test series (which comprised 7 of the 9 experiments performed) were selected for assessment – see Table 7. The selected tests include a common congestion/confinement arrangement, enabling the performance of EXSIM for various hydrogen-air mixture stoichiometries to be directly evaluated.

Table 7: Summary of selected cases for modelling

Experiment ID	Congestion Arrangement	Stoichiometric Ratio
Hydrogen06	4-Gate	0.967
Hydrogen07	4-Gate	0.969
Hydrogen08	4-Gate	1.226
Hydrogen10	4-Gate	1.711
Hydrogen11	4-Gate	0.800
Hydrogen15	4-Gate	1.253

3.9.2 Model setup details

3.9.2.1 Geometry

The test rig geometry was manually constructed for use with EXSIM. An example model snapshot is shown in Figure 27.

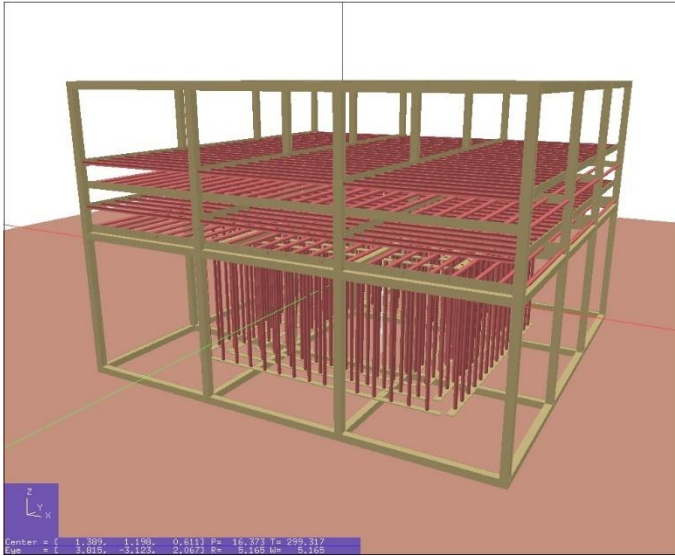


Figure 27: EXSIM 3D model for the Shell/HSL hydrogen repeated pipe congestion tests

3.9.2.2 Gas composition

Hydrogen was selected as the fuel gas for all cases, with the stoichiometric ratio for each test case specified in accordance with Table 7.

3.9.2.3 Fill fraction

In alignment with the experimental configuration, a 100% fill of the test rig was defined within the model for all cases.

3.9.2.4 Ignition

A single ignition location, located centrally within the test rig at an elevation of 0.5 m, was used for all 5 tests.

3.9.2.5 Data monitoring

The test rig was fitted with 5 pressure transducers mounted at increasing distances from the ignition point, 0.5 m above ground level. A further series of transducers were positioned externally at varying distances from the rig boundary (up to approximately 30.5 m) at heights ranging from 0.5 m to 4.4 m.

The validation exercise considered measurements taken from the internally located transducers *exclusively*.

3.9.2.6 Computational mesh

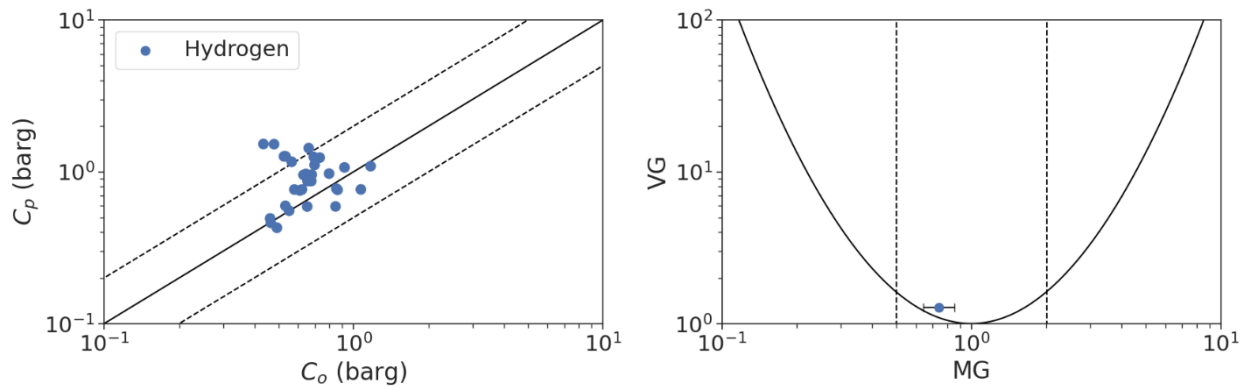
The mesh within the core combustion zone was defined as per the recommendations from EXSIMPOR. In all cases, this corresponded to cells of approximately 0.20 m in size. Beyond the region of interest, the cell size was allowed to grow with an expansion factor of 1.05.

3.9.2.7 Boundary conditions

The ground boundary (-z) was set to 'solid' for all cases, with all other boundaries set to 'open'.

3.9.3 Results

A summary of the results obtained for direct point-by-point 'peak pressure' comparisons of the modelled Shell/HSL Hydrogen Repeated Pipe Congestion cases are presented in Figure 28, below. Comparisons between experimental observation and model prediction via the 'max. of peak' measure (see Section 2.4) are provided in Figure 29.

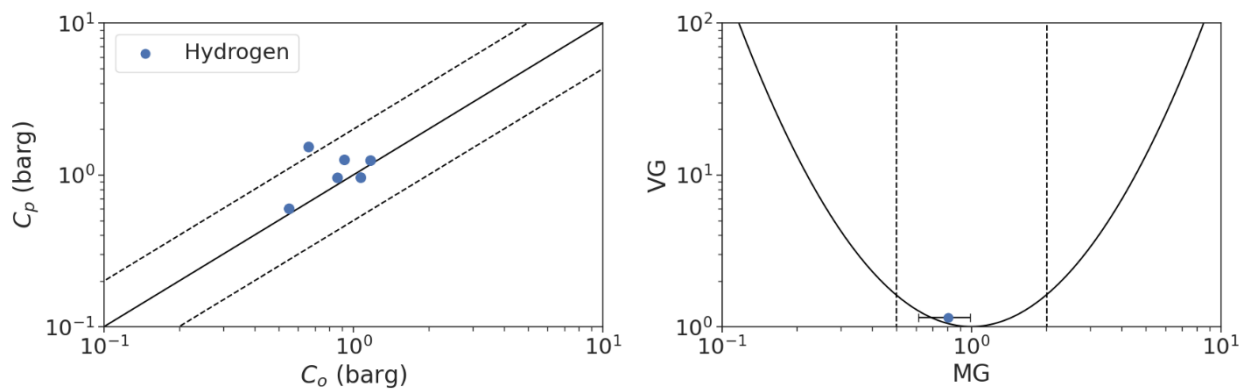


MG	95% CI ^{Note 1}	VG	FAC2
0.74	[0.64, 0.85]	1.29	0.80

Notes:

Note 1 – 95% confidence interval (CI) for MG

Figure 28: Validation results obtained for modelled Shell/HSL hydrogen repeated pipe congestion cases (direct point-by-point comparison)



MG	95% CI ^{Note 1}	VG	FAC2
0.81	[0.61, 0.99]	1.15	0.83

Notes:

Note 1 – 95% confidence interval (CI) for MG

Figure 29: Validation results obtained for modelled Shell/HSL hydrogen repeated pipe congestion cases ('max. of peak' comparison)

The following key observations were made based on the results:

- The results indicate that the code's predictions are in good agreement with the experimental data, with a tendency to overpredict for higher stoichiometric ratios.
- The code correctly captured the observed trends as the stoichiometric ratio was varied, predicting higher pressures for ratios closer to the optimum values.

3.10 FM Global vented hydrogen explosion tests

3.10.1 Description and case selection

This experimental programme, performed by FM Global, sought to explore the influence of a range of parameters (including hydrogen concentration, ignition location, vent size and congestion) on the pressure development of a propagating flame in a vented enclosure [20].

The test series considered pre-mixed, hydrogen gas explosions within a vented, cuboidal enclosure of dimensions 4.6 m x 4.6 m x 3.0 m (yielding an overall internal volume of approximately 63.5 m³) – see Figure 30. A selection of lean hydrogen-air mixtures, with hydrogen concentrations in the range 12-19%, were examined in tandem with up to three ignition locations and two venting configurations. Whilst the vast majority of the tests were performed without any obstacles present within the chamber, a small subset included an array of square cross-sectioned vertical pillars.

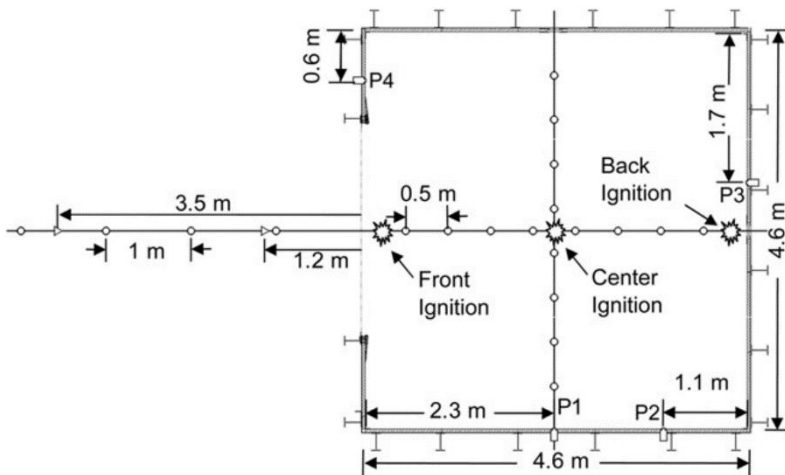


Figure 30: Plan view of test chamber [20]

As shown in Table 8, 18 tests from the overall experimental campaign were selected for assessment. The selected tests cover a range of hydrogen concentrations, ignition locations and vent sizes.

Table 8: Summary of selected cases for modelling

Test No.	Hydrogen Concentration (%)	Ignition Position	Vent Size (m ²)	Congestion
1	12.10	Centre	5.4	None
2	14.90	Centre	5.4	None
3	16.50	Centre	5.4	None
4	18.00	Centre	5.4	None
5	18.10	Centre	5.4	None
6	19.00	Centre	5.4	None
7	19.10	Centre	5.4	None
8	19.70	Centre	5.4	None

Test No.	Hydrogen Concentration (%)	Ignition Position	Vent Size (m ²)	Congestion
9	17.50	Centre	2.7	None
10	18.00	Centre	2.7	None
14	16.50	Back Wall	5.4	None
15	17.20	Back Wall	5.4	None
16	17.90	Back Wall	5.4	None
17	18.30	Back Wall	5.4	None
18	19.00	Back Wall	5.4	None
19	15.10	Back Wall	2.7	None
20	17.10	Back Wall	2.7	None
21	17.80	Back Wall	2.7	None

3.10.2 Model setup details

3.10.2.1 Geometry

The cuboidal test chamber (dimensions 4.6 m x 4.6 m x 3.0 m) was vented in all tests via a square opening (with an area of either 2.7 m² or 5.4 m²) positioned centrally on one of the vertical walls.

A full-scale 3D model of the enclosure was constructed for each venting configuration of interest. A model snapshot showing the utilised 3D model for the 5.4 m² case is presented in Figure 31.

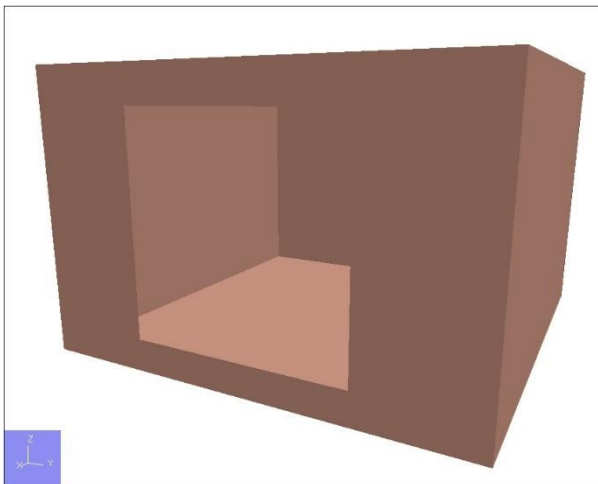


Figure 31: Example EXSIM 3D model of the FM Global test chamber (vent area = 5.4 m²)

3.10.2.2 Gas composition

Hydrogen was selected as the fuel gas for all cases, with the equivalence ratio for each test case specified in accordance with Table 9 (based on an assumed stoichiometric concentration for hydrogen-air mixtures of 29.5%).

Table 9: Equivalence ratios for each test case

Test No.	Hydrogen Concentration (%)	Equivalence Ratio
1	12.10	0.41
2	14.90	0.51
3	16.50	0.56
4	18.00	0.61
5	18.10	0.61
6	19.00	0.64
7	19.10	0.65
8	19.70	0.67
9	17.50	0.59
10	18.00	0.61
14	16.50	0.56
15	17.20	0.58
16	17.90	0.61
17	18.30	0.62
18	19.00	0.64
19	15.10	0.51
20	17.10	0.58
21	17.80	0.60

3.10.2.3 Fill fraction

In alignment with the experimental configuration, a 100% fill of the module was defined within the model for all cases.

3.10.2.4 Ignition

A total of two ignition locations were considered within the selected set of experiments:

- One at the centre of the test chamber; and
- One at the centre of the rear wall of the test chamber.

3.10.2.5 Data monitoring

The test rig was fitted with 4 pressure transducers mounted to the chamber walls at an elevation of 2.3 m (see Figure 30). A further two transducers were mounted externally at varying distances from the vent atop of 0.3 m high concrete slab

The validation exercise considered measurements taken from the internally located transducers *exclusively*.

3.10.2.6 Computational mesh

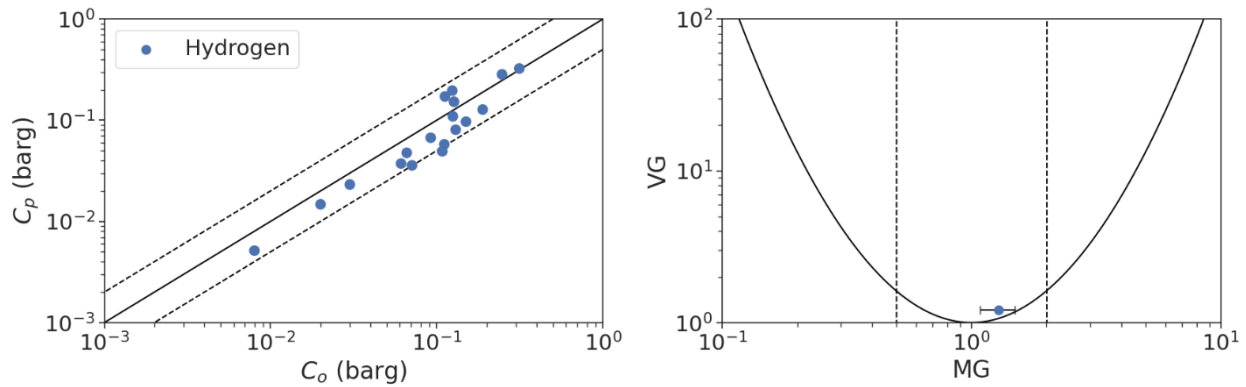
The mesh within the core combustion zone was defined as per the recommendations from EXSIMPOR. In all cases, this corresponded to cells of approximately 0.37 m in size. Beyond the region of interest, the cell size was allowed to grow with an expansion factor of 1.1.

3.10.2.7 Boundary conditions

The ground boundary (-z) was set to 'solid' for all cases, with all other boundaries set to 'open'.

3.10.3 Results

A summary of the 'max. of peak' pressure results obtained for the FM Global Vented Hydrogen Explosion test series is presented in Figure 32, below.



MG	95% CI ^{Note 1}	VG	FAC2
1.28	[1.08, 1.50]	1.21	0.94

Notes:

Note 1 – 95% confidence interval (CI) for MG

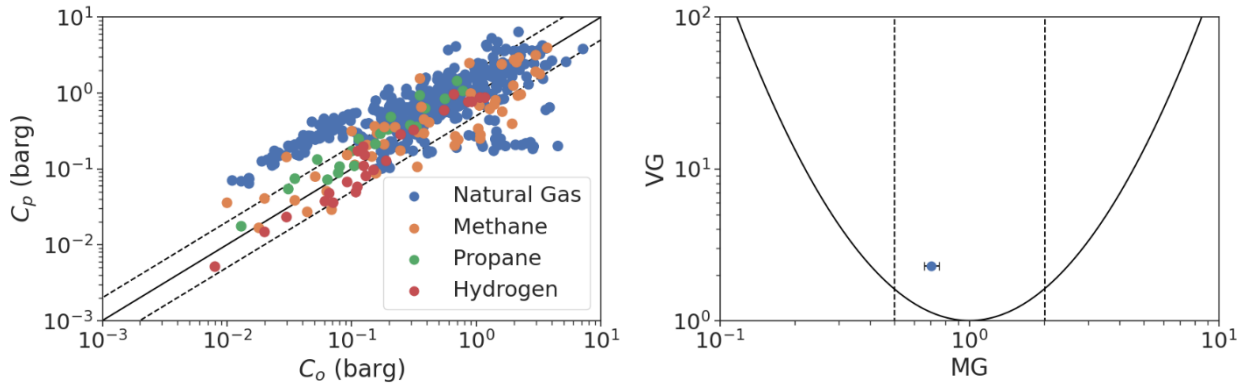
Figure 32: Validation results obtained for FM Global vented hydrogen test cases

The following key observations were made based on the results:

- The results indicate that the code's predictions are in good agreement with the experimental data, showing a slight tendency to underpredict.
- The code correctly captured the observed trends as the stoichiometric ratio was varied, predicting higher pressures for ratios closer to the optimum values and ignition towards the cloud edges.
- Overall, 94% of the EXSIM predictions were assessed to be within a factor of 2 of the experimental result.

4 SUMMARY OF MODEL PERFORMANCE

EXSIM's overall performance, taking the complete library of validation cases into account, is summarised in Figure 33. By default, the plot includes full point-by-point 'peak pressure' comparisons between individual transducers readings and their associated predicted values; where such data are not available, comparisons of observed and predicted pressures via the 'max. of peak' measure are included as an alternative (see Section 2.4).



MG	95% CI ^{Note 1}	VG	FAC2
0.70	[0.66, 0.76]	2.30	0.62

Notes:

Note 1 – 95% confidence interval (CI) for MG

Figure 33: Validation results obtained for all cases combined

The results show that the code generally performs well across the full range of analysed scales, geometries and gas types when models are set up in alignment with the stipulated guidelines [11]. For the modelled cases, the prediction quality can typically be seen to be good across a broad range of observed pressure levels, with a tendency towards overprediction for lower pressures.

5 REFERENCES

1. Hjertager BH, Solberg T and Nymoer KO. Computer modelling of gas explosion propagation in offshore modules. *J. Loss Prev. Process Ind.* 1992; 5(3):165-174.
2. Hjertager BH. Computer Modelling of Turbulent Gas Explosions in Complex 2 and 3D Geometries. *J. Hazardous Materials.* 1993; 34:173-197.
3. Sæter O, Solberg T and Hjertager BH. Validation of the EXSIM-94 Gas Explosion Simulator. Proceedings of the 4th International Conference on Offshore Structures – Hazards, Safety and Engineering, London, UK. 1995.
4. Sæter O. Modelling and simulation of gas explosions in complex geometries [dissertation]. Trondheim, Norway: NTNU; 1998.
5. Mogensen S, Hjertager BH. and Solberg T. Investigation of Gas Explosions in Open Geometries using EXSIM. Int. Conf. and Workshop on Modeling the Consequences of Accidental Releases of Hazardous Materials, San Francisco, USA. 1999.
6. Hjertager, BH, Solberg T. A review of computational fluid dynamics modeling of gas explosions. *Prevention of hazardous fires and explosions.* Kluwer Publ.; 1999. p.77-91.
7. Rian K *et al.* Coherent computational analysis of large-scale explosions and fires in complex geometries – from combustion science to a safer oil and gas industry. *Chemical Engineering Transactions.* 2016; 48:175-180
8. Mekonnen AT. Modeling and numerical simulation of gas explosions for industrial safety analyses [master's thesis]. Porsgrunn, Norway: Telemark College; 2019.
9. Hanna SR, Messier LL, Schulman LL. Hazard Response Modeling Uncertainty (A quantitative method): Final Report. Lexington MA, USA: Sigma Research Corporation; 1988.
10. Model Evaluation Group Gas Explosions (MEGGE). Gas Explosion Model Evaluation Protocol: Technical Report, Version 1. 1996.
11. DNV. EXSIM V6.0: EXSIM User Manual; 2023.
12. Hanna S, Chang J. Air quality model evaluation. *Meteorol. Atmos. Phys.* 2004; 87(1-3):167-196.
13. Efron B. The Jackknife, The Bootstrap and other Resampling Plans. *Soc. Ind. and Appl. Math.*; 1982.
14. BG Technology. Explosions in Full Scale Offshore Module Geometries – Main Report. UK HSE Offshore Technology Report OTO 1999 043; 2000.
15. Johnson M. Understanding of Gas Explosions: The Importance of Experimental Research. *Fire and Blast Information Group (FABIG) Newsletter, Issue 62.* FABIG; 2013 p.4-8.
16. Hansen OR, Johnson DM. Improved far-field blast predictions from fast deflagrations, DDTs and detonations of vapour clouds using FLACS CFD. *J. Loss Prev. Process Ind.* 2015; 35:293-306.
17. Advantica Technology. Gas Explosions in Offshore Modules Following Realistic Releases (Phase 3B): Final Summary Report. Report No. R4853, Issue 1, 2002.
18. Tomlin G *et al.* The effect of vent size and congestion in large-scale vented natural gas/air explosions. *J. Loss Prev. Process Ind.* 2015; 35:169-181.
19. Shirvill LC *et al.* Experimental study of hydrogen explosion in repeated pipe congestion – Part 1: Effects of increase in congestion. *Int. J. Hydrogen Energy* 2019; 44:9466-9483.
20. Bauwens CR, Chao J, Dorofeev SB. Effect of hydrogen concentration on vented explosion overpressures from lean hydrogen-air deflagrations. *Int. J. Hydrogen Energy* 2012; 37:17599-17605.



About DNV

We are the independent expert in risk management and quality assurance. Driven by our purpose, to safeguard life, property and the environment, we empower our customers and their stakeholders with facts and reliable insights so that critical decisions can be made with confidence. As a trusted voice for many of the world's most successful organizations, we use our knowledge to advance safety and performance, set industry benchmarks, and inspire and invent solutions to tackle global transformations.

Digital Solutions

DNV is a world-leading provider of digital solutions and software applications with focus on the energy, maritime and healthcare markets. Our solutions are used worldwide to manage risk and performance for wind turbines, electric grids, pipelines, processing plants, offshore structures, ships, and more. Supported by our domain knowledge and Veracity assurance platform, we enable companies to digitize and manage business critical activities in a sustainable, cost-efficient, safe and secure way.